

Deformation at ambient and high temperature of *in situ* Laves phases-ferrite composites

Patricia Donnadieu¹, Carsten Pohlmann^{2,4}, Sergio Scudino²,
Jean-Jacques Blandin¹, Kumar Babu Surreddi^{2,5} and Jürgen Eckert^{2,3}

¹Laboratoire SIMaP, CNRS—Université de Grenoble, F-38402 Saint Martin d'Hères, France

²IFW Dresden, Institut für Komplexe Materialien, Postfach 27 01 16, D-01171 Dresden, Germany

³TU Dresden, Institut für Werkstoffwissenschaft, D-01062 Dresden, Germany

E-mail: patricia.donnadieu@simap.grenoble-inp.fr

Received 16 January 2014

Accepted for publication 2 May 2014

Published 29 May 2014

Abstract

The mechanical behavior of a $\text{Fe}_{80}\text{Zr}_{10}\text{Cr}_{10}$ alloy has been studied at ambient and high temperature. This $\text{Fe}_{80}\text{Zr}_{10}\text{Cr}_{10}$ alloy, whose microstructure is formed by alternate lamellae of Laves phase and ferrite, constitutes a very simple example of an *in situ* CMA phase composite. The role of the Laves phase type was investigated in a previous study while the present work focuses on the influence of the microstructure length scale owing to a series of alloys cast at different cooling rates that display microstructures with Laves phase lamellae width ranging from ~ 50 nm to ~ 150 nm. Room temperature compression tests have revealed a very high strength (up to 2 GPa) combined with a very high ductility (up to 35%). Both strength and ductility increase with reduction of the lamella width. High temperature compression tests have shown that a high strength (900 MPa) is maintained up to 873 K. Microstructural study of the deformed samples suggests that the confinement of dislocations in the ferrite lamellae is responsible for strengthening at both ambient and high temperature. The microstructure scale in addition to CMA phase structural features stands then as a key parameter for optimization of mechanical properties of CMA *in situ* composites.

Keywords: complex metallic alloys, metal matrix composites, *in situ* composites, mechanical behavior


1. Introduction

Complex metallic alloys (CMA) has become the generic name for many intermetallic phases having common structural features at the atomic level and also some macroscopic properties [1]. This class of intermetallic alloys includes quasicrystals as well as phases earlier called Frank–Kasper

phases [2] or alternatively topologically closed packed phases [3]. The major structural feature of CMA phases is that they cannot be described as a variation on simple cubic or hexagonal structures since their atomic decoration is based on a local compact packing of atoms forming icosahedral clusters or larger clusters related to an initial icosahedra. Such atomic motives frequently lead to crystals with large cell, as for instance the so-called Samson phase ($\beta\text{Mg}_2\text{Al}_3$, ~ 1200 atoms/cell) [4], or even larger, as reported in the Al–Ta–Cu system [5]. However also some CMA phases with smaller cell exist; the CMA phases with the smallest cells are described by the Laves phase structure type, the so-called C15, C14 and C36 phases. These phases are not rare; on the contrary they correspond to several thousand of alloys [6]. In addition to the common structural features, the CMA phases have in

⁴ Present address: Fraunhofer-Institut f. Fertigungstechnik und Angewandte Materialforschung, IFAM Institutsteil Dresden, D-01277 Dresden, Germany.

⁵ Present address: Department of Materials and Manufacturing Technology, Chalmers University of Technology, SE-41296 Göteborg, Sweden.

 Content from this work may be used under the terms of the Creative Commons Attribution-NonCommercial-ShareAlike 3.0 licence. Any further distribution of this work must maintain attribution to the author(s) and the title of the work, journal citation and DOI.

common some mechanical properties: they are extremely hard at room temperature but exhibit a high deformability at high temperature [7–9].

Although CMA phases possess remarkable structural and physical properties and are frequent in metallurgy, their applications remain limited because of the high brittleness that accompanies their high strength. Indeed, this drawback can be overcome if the CMA phases are considered as reinforcing phases for metallic matrix composites. Such composites can be conveniently produced by powder metallurgy. For instance, in Al based systems, a series of composite containing high content of CMA phases have been obtained that were exhibiting remarkable high strength and ductility [10]. However, as CMA phases are metallic systems that can be frequently found in equilibrium with simple alloys (for instance Fe, Al, Cr or Mg), it is then also possible to obtain *in situ* composites. For instance in the Ni–Al–Ta system, composites prepared either by powder metallurgy and solidification have been designed in view of applications requiring high levels of mechanical properties [11–14]. Still, a conventional process like casting has the advantage on powder metallurgy to give composites with coherent and chemically stable interfaces. *In situ* composites containing Laves phases and a simple alloy can be produced by solidification; moreover, due to the abundance of Laves phases, a eutectic mixture is frequently obtained. For instance, in binary alloy, eutectic ferrite-Fe₂Ti Laves phase alloys can be obtained [15]; interestingly in the ternary Fe_{90-x}Zr₁₀Cr_x alloys a series of eutectic mixtures can be synthesized that are formed by ferrite and either the C15 Laves or the C14/C36 Laves phases depending on the Cr content [16]. For both the Fe–Ti and Fe–Zr–Cr systems, the alloys display a microstructure of alternating ferrite and Laves phase lamellae and exhibit a good combination of strength and ductility at room temperature. Similar behavior was reported for eutectic–dendrite composites from the binary Fe–Zr [17], Ni–Zr [18] and Fe–Nb [19] systems. These materials were produced by copper mold casting, which is characterized by cooling rates of the order of 10–100 K s⁻¹, and contained nanocrystalline eutectic structures [20]. The application of such a high cooling rate limits grain growth, consequently promoting the formation of nanocrystalline microstructures through the reduction of the eutectic lamellar spacing. Hence, solidification using copper mold casting appears to be as a very simple method to study the effect of the microstructure scale on the eutectic Laves phase composites.

In a previous work on the Fe–Zr–Cr alloys [16], we have shown that owing to the composition choice (Fe₈₀Zr₁₀Cr₁₀) it was possible to favor the formation of the hexagonal C14/C36 Laves phase instead of the cubic C15 Laves phases and further improve significantly the ductility. In view of pushing further the optimization of these *in situ* composites, changing the microstructure scale appears as another option to investigate. The present work will report first on the room temperature mechanical behavior of Fe₈₀Zr₁₀Cr₁₀ alloy solidified at different cooling rates. To have more complete description of the mechanical behavior, high temperature compression tests will also be reported in the present study. The

mechanical behavior study will be complemented by a microstructural study of the deformed samples in order to identify the mechanisms responsible for strengthening at ambient and high temperature. The potential of CMA phase *in situ* composites with respect to the optimization of mechanical properties will be discussed on the basis of our results.

2. Experimental details

Ingots with nominal compositions Fe₈₀Zr₁₀Cr₁₀ (purity > 99.9 wt%) were prepared by arc melting in a titanium-gettered argon atmosphere. The ingots were remelted several times in order to achieve a homogeneous master alloy. From these ingots, cylindrical bulk samples with different diameters ($\Phi = 1, 2, 3$ and 4 mm) and 80 mm length were prepared by copper mold casting. According to a previous study [16], for nominal composition Fe₈₀Zr₁₀Cr₁₀, the as-cast material is composed of essentially two phases: ferrite and hexagonal C14/C36 Laves phases; C15 Laves phase can be present at a minor level. Phase analysis was carried out by x-ray diffraction (XRD) to check for the presence of the expected phases using a STOE Stadi P diffractometer (Mo-K α_1 radiation). The Rietveld method was applied for the structure refinement using the WinPlotR software package [21]. The microstructure was investigated by scanning electron microscopy (SEM) coupled with energy-dispersive x-ray (EDX) analysis (Jeol JSM 6400 microscope) and by transmission electron microscopy (TEM) using a Jeol 3010 microscope operating at 300 keV. TEM samples were prepared from the $\Phi = 2, 3$ and 4 mm rods by mechanical polishing followed by ion milling with Ar⁺ ion accelerated at 4 keV. The $\Phi = 1$ mm rods were too difficult to handle to allow for this classical specimen preparation, TEM sections were then obtained by focussed ion beam (FIB) machining. Cylindrical specimens with aspect ratio length : diameter of 2 : 1 were prepared from the as-cast rods with different diameters and mechanically tested at room temperature with an INSTRON 8562 facility under quasistatic loading (strain rate of 5×10^{-5} to 1×10^{-4} s⁻¹). Both ends of the specimens were polished to make them parallel to each other prior to the compression test. Samples for compression testing were cut with a diamond wire saw in the $\Phi = 4$ mm diameter alloy in shape of a cylinder with a height of 5 mm. Compression tests were carried out at 873 K and 1273 K with MTS—4M equipment (strain rate 5×10^{-5} s⁻¹). Heating rates close to 10 K min⁻¹ were applied to reach the desired testing temperature. Specimens were homogenized for 10 min before compression testing.

3. Results

3.1. Microstructure of the as-cast samples

Figure 1(a) shows the XRD patterns of the as-cast Fe₈₀Zr₁₀Cr₁₀ rods with different mold diameter. The patterns of all the samples display sharp diffraction peaks

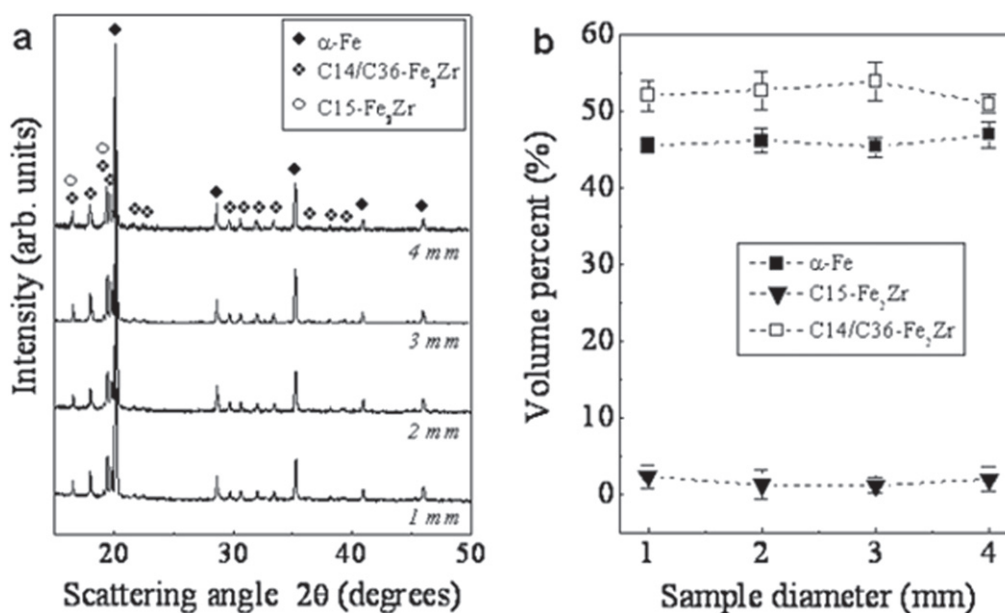


Figure 1. (a) XRD patterns (Mo radiation) of the as-cast $\text{Fe}_{80}\text{Zr}_{10}\text{Cr}_{10}$ alloys cast with different cooling rates (mold diameter $\phi = 1, 2, 3, 4$ mm). (b) Volume fractions of the different phases evaluated by Rietveld structure refinement for the alloy series ($\phi = 1, 2, 3, 4$ mm). No influence of the cooling rate on the volume fractions of the phases is observed.

corresponding to the body-centered cubic (bcc) α -Fe phase. In addition, several reflections consistent with both the hexagonal polymorphs (C14 or C36) of the Fe_2Zr Laves phase structure can be observed. As already reported for the $\text{Fe}_{80}\text{Zr}_{10}\text{Cr}_{10}$ sample ($\phi = 4$ mm mold diameter) [16], the samples also contain a small amount (about 2 vol%) of the cubic (C15) polymorph of the Fe_2Zr Laves phase [6]. Figure 1(b) shows the volume fractions of the different phases as a function of the sample diameter evaluated by the Rietveld structure refinement. The results indicate that the variation of the cooling rate does not significantly affect the relative amounts of the different phases in the $\text{Fe}_{80}\text{Zr}_{10}\text{Cr}_{10}$ rods (α -Fe ~ 46 vol%; C14/C36 ~ 52 vol%; C15 ~ 2 vol%).

The SEM and TEM images in figure 2 illustrate typical microstructures of the $\text{Fe}_{80}\text{Zr}_{10}\text{Cr}_{10}$ alloy cast in the $\phi = 4$ mm mold. The SEM images (figures 2(a), (b)) show that the microstructure consists of Laves phase particles with sizes ranging between 2 and 5 μm formed in the first solidification stage embedded in a eutectic mixture. The particle composition measured by EDX analysis is $\text{Fe}_{68}\text{Zr}_{27}\text{Cr}_5$ which is in agreement with the lower value (20 at%) reported for the Zr content in the hexagonal Laves phase [22].

According to TEM (figure 2(c)), the eutectic mixture is formed of alternate submicronic lamellae of ferrite and Laves phases. For the $\phi = 4$ mm diameter sample, the lamella sizes are respectively ~ 100 nm for the Laves phase and ~ 150 nm for the ferrite. For smaller mold diameters, the alloy displayed similar microstructures. However, as illustrated by the TEM images in figure 3, smaller lamella widths are observed when the diameter is reduced: namely for the $\phi = 2$ mm alloy, typical sizes were ~ 80 nm for the Laves phase lamellae and ~ 100 nm for the ferrite one; for the $\phi = 1$ mm alloy, typical sizes were ~ 50 nm for the Laves phase and ~ 70 nm for ferrite lamellae.

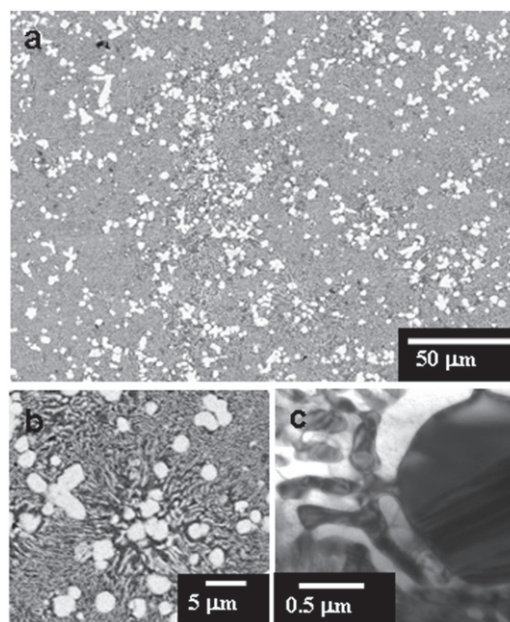


Figure 2. (a) SEM image of the as-cast $\text{Fe}_{80}\text{Zr}_{10}\text{Cr}_{10}$ rod corresponding to casting in the $\phi = 4$ mm diameter mold. The SEM image being formed with back scattered electrons (BSE) the Laves phases have a contrast brighter than ferrite. (b) High magnification SEM view showing the Laves phase particles and the eutectic mixture (c) bright field (BF). TEM image of a Laves phase particle embedded in the eutectic mixture formed by alternate Laves phases and ferrite lamellae. Note that on BF TEM image the Laves phase has a contrast darker than ferrite due to a stronger diffraction effect.

3.2. Room temperature deformation and microstructure of the deformed samples

The series of $\text{Fe}_{80}\text{Zr}_{10}\text{Cr}_{10}$ rods cast at different cooling rates were further tested by compression at room temperature. The

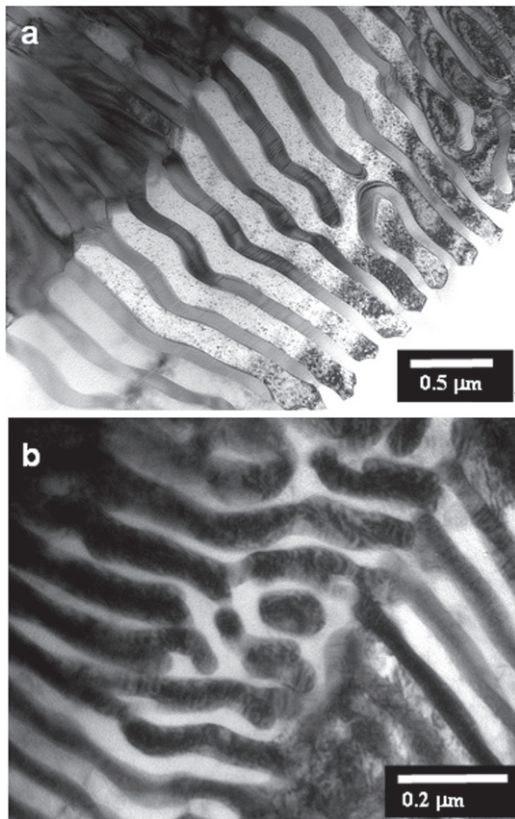


Figure 3. Lamellar eutectic microstructure of the $\text{Fe}_{80}\text{Zr}_{10}\text{Cr}_{10}$ alloy cast in the $\Phi = 2$ mm diameter mold (figure 3(a)) and of the alloy cast in the $\Phi = 1$ mm diameter mold (figure 3(b)). The lamella scale is changed by a factor of approximately 1.5 (a) width ~ 80 nm for Laves phases and ~ 100 nm for ferrite lamellae; (b) width ~ 50 nm for the Laves phase and ~ 70 nm for ferrite lamellae. In all as-cast states, the Laves phase lamellae often show a striated contrast due to a high density of native planar defects. Note that the TEM image in figure 3(b) was obtained on a FIB section, the mottled contrast observed in this case results from an FIB redeposition artifact.

uniaxial compression stress–strain curves are shown in figure 4(a). For all casting conditions, the samples display a remarkable deformation behavior: high strength with high strain. For the $\Phi = 4$ mm alloy, the specimen exhibits a compressive strength of about 1.8 GPa combined with a plastic strain exceeding 15%. The compressive strength is even higher with higher strain for the $\Phi = 2$ mm and $\Phi = 1$ mm alloys: strength of more than 2 GPa for a strain larger than 30% and than 35%, respectively. In fact, we note a significant evolution of strain and stress with cooling rate, i.e. the mold diameter (figure 4(b)): both strength and strain increase with increasing cooling rate. In other words strength does not increase at the expense of a reduction of ductility. According to the Hall–Petch law, the yield stress varies as an inverse of the square root of the grain size. In the present case, we have plotted the compressive strength as a function of the inverse of the lamella size. The graph in figure 4(c) shows that a linear dependence can be found (ordinate at origin: 1700 MPa). However the stress range being limited and the error bars on size rather large, this linear dependence indicates only a qualitative agreement with the Hall–Petch law.

To identify the deformation mechanisms, TEM observations (figures 5(a) and (b)) were carried out on deformed samples corresponding respectively to the $\Phi = 4$ mm and $\Phi = 2$ mm casting conditions. For the $\Phi = 4$ mm deformed sample, the bright field image in figure 5(a) shows that dislocations are present only in the ferrite lamellae. The Laves phase lamellae do not show any defects, except the planar native defects already present in as-cast states (see figures 2(c), 3) and already mentioned in a previous work [16]. For the $\Phi = 2$ mm deformed sample, bright field imaging was not appropriate due to the high level of deformation that gives a very unclear image. Here dark field imaging provides a more appropriate contrast that reveals a high density of dislocations located in the ferrite lamellae. According to the TEM image contrast, the dislocation density is higher in the $\Phi = 2$ mm deformed sample than in the $\Phi = 4$ mm one. This higher density of dislocations is consistent with the higher strain of the $\Phi = 2$ mm sample compared to the $\Phi = 4$ mm one. The ferrite lamella size reduction (~ 100 nm for $\Phi = 2$ mm sample, ~ 150 nm for $\Phi = 4$ mm sample) suggests that the strength increase is due to the confinement of dislocations in smaller channels.

The absence of evidence for dislocations in the Laves phase lamellae is in agreement with our previous work [16] showing that for the C14/36 Laves phase lamellae, shearing did not occur while for the cubic C15 Laves phase lamellae were sheared by dislocations with further localized shearing and fracture. In the $\Phi = 4$ mm C14/36 Laves phase composite, the damages responsible for rupture result from the opening of large voids at the interface (figure 6(a)). In some areas of the $\Phi = 2$ mm C14/36 Laves phase composite showing lamellae with a very small thickness (~ 30 nm), we have observed the formation of voids across the Laves phase lamellae (figure 6(a)). Hence at that lamella size the C14/36 Laves phase lamellae behave as the C15 Laves phase lamellae. We interpret then this type of damage as the result of the localization of deformation in the C14/36 Laves phase lamellae that has become shearable at very small size.

3.3. High temperature deformation and microstructure of the deformed samples

To investigate the high temperature mechanical behavior, compression tests have been carried out on the $\text{Fe}_{80}\text{Zr}_{10}\text{Cr}_{10}$ alloy cast in the $\Phi = 4$ mm mold. The samples were deformed by 15% at 873 K and 1273 K. Figures 7(a) and (b) display the stress–strain curves for deformation at 873 K and 1273 K, respectively. Remarkably, at 873 K the maximum stress is still high (900 MPa); at 1273 K the maximum stress is only 40 MPa.

TEM observations carried out on the deformed samples are reported in figure 8. Figure 8(a) shows a DF TEM image of the sample deformed at 873 K (figure 8(a)). Even though the specimen was held at 873 K for ~ 2 h, one can recognize a lamellar microstructure similar to the as-cast state (figure 1(b)) which indicates no significant evolution of the microstructure due to thermal effects at this temperature. In this deformed state, we observed that there were no traces of

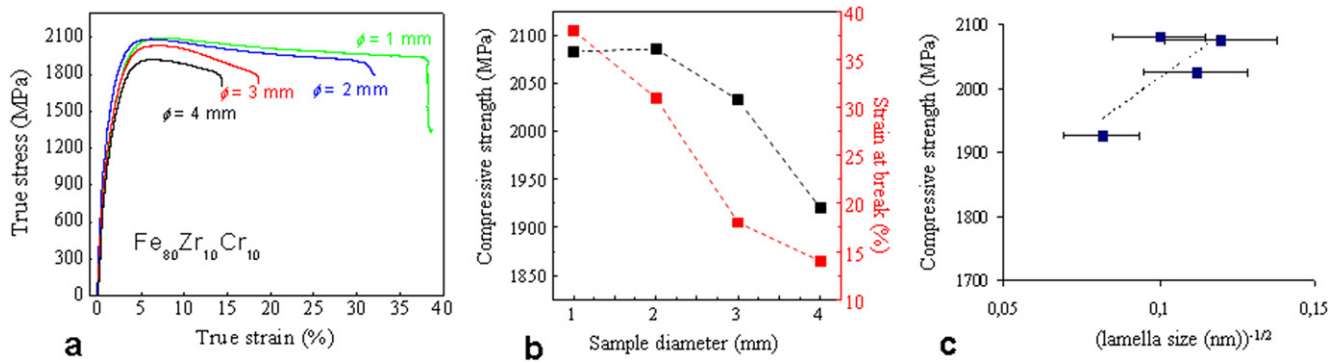


Figure 4. (a) Room temperature compression true stress–true strain curves for the Fe₈₀Zr₁₀Cr₁₀ alloys as a function of their respective cooling conditions (Φ = 1, 2, 3, 4 mm). (b) Variations of strength (maximum compressive stress) and ductility (strain at break) as a function of cooling conditions. (c) Hall–Petch type plot: compressive strength as a function of (lamella size)^{-1/2} for the sample series (Φ = 1, 2, 3, 4 mm).

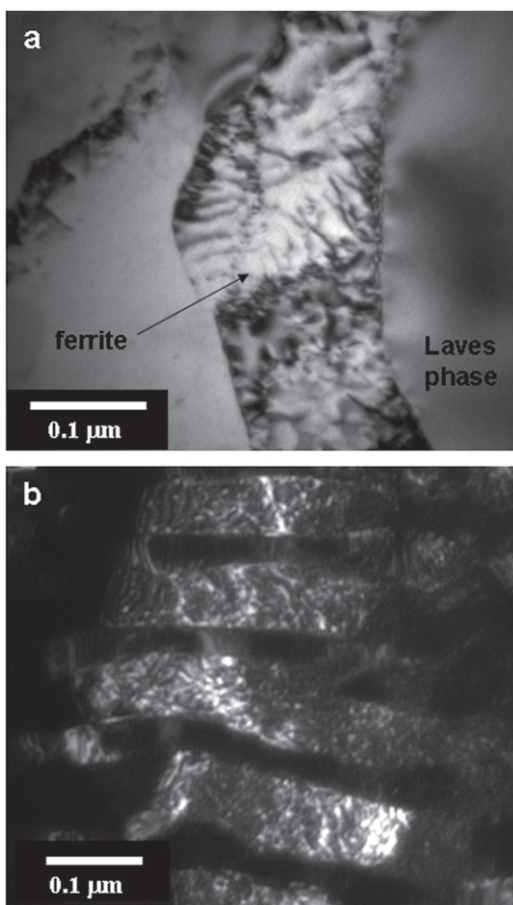


Figure 5. (a) Microstructure of the deformed Fe₈₀Zr₁₀Cr₁₀ alloy cast in the Φ = 4 mm diameter mold. The BF TEM image clearly shows dislocations in the ferrite lamellae and absence of dislocations in the neighboring Laves phase lamellae. (b) Microstructure of the deformed Fe₈₀Zr₁₀Cr₁₀ alloy cast in the Φ = 2 mm diameter mold. The DF TEM image displays a mottled contrast corresponding to a high density of dislocations in the ferrite lamellae while the Laves phase lamellae in dark contrast do not show dislocations.

dislocations in the Laves phase lamellae but many dislocations in the ferrite lamellae. Hence, at 873 K, the microstructure of the deformed samples displays the same feature as that of samples deformed at room temperature: dislocations

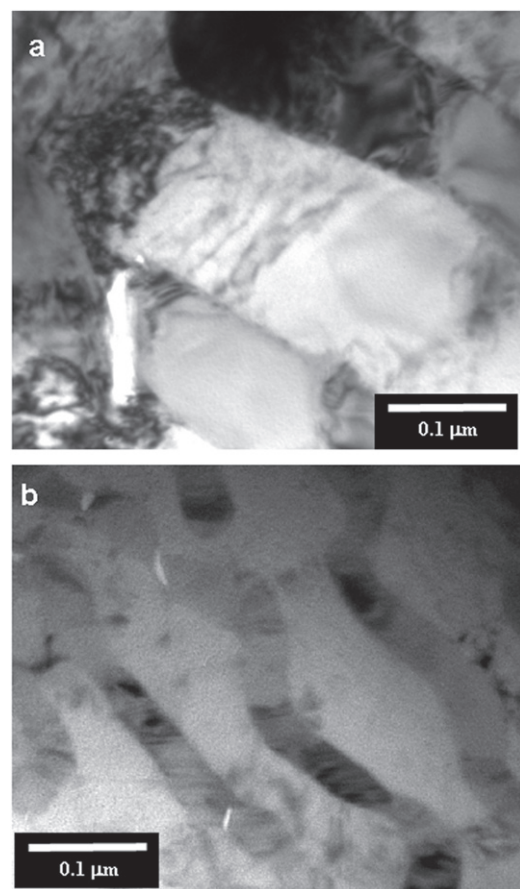


Figure 6. (a) Void formation at the interface between Laves phases and ferrite in a Φ = 4 mm deformed sample (area close to fracture). (b) Zone with very small lamellar size (~30 nm) in a Φ = 2 mm deformed sample (area close to fracture) showing the formation of voids across the Laves phase lamellae.

are confined in the ferrite lamella. Regarding the sample deformed at 1273 K (figure 8(b)), a significant coarsening can be noticed. Complementary TEM observations (not reported here) of samples annealed for 1h at 1273 K indicate a similar coarsening. Under heat treatment at 1273 K, the microstructure is similar to the one shown in figure 8(b); the Laves phase part forms either globular or roughly lamellar shape

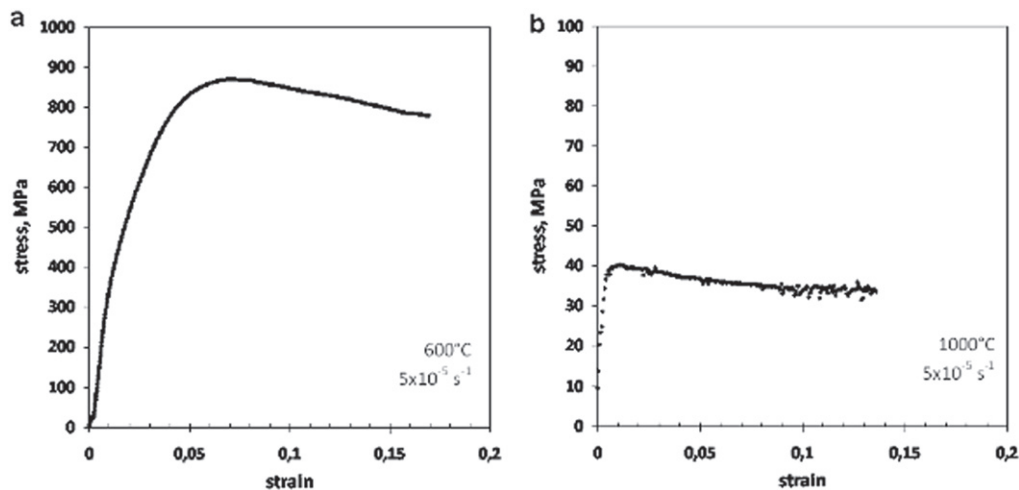


Figure 7. Mechanical behavior at high temperature of a $\text{Fe}_{80}\text{Zr}_{10}\text{Cr}_{10}$ alloy cast in the $\Phi=4$ mm diameter mold: (a) compression test at 873 K and (b) compression test at 1273 K.

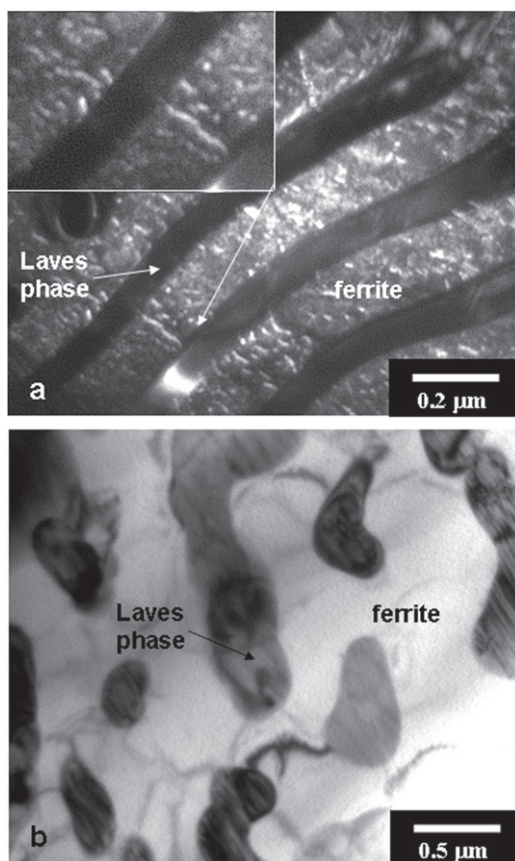


Figure 8 (a) Microstructure of the $\text{Fe}_{80}\text{Zr}_{10}\text{Cr}_{10}$ alloy deformed by 15 % at 873 K. The DF TEM image shows a high density of dislocation confined in the ferrite lamellae. (b) Microstructure of the $\text{Fe}_{80}\text{Zr}_{10}\text{Cr}_{10}$ alloy deformed by 15 % at 1273 K. The lamellar microstructure has significantly coarsened. Contrary to the sample deformed at 873 K no dislocation were observed.

particles with a typical width of about $0.5 \mu\text{m}$ while the ferrite part has completely lost its lamellar type microstructure. Regarding deformation, in the ferrite part only some bend contours are observed but no dislocations.

These observations suggest that the high strength is maintained at 873 K because of the confinement of deformation in the ferrite lamellae. At 1273 K, due to the coarsening of the lamellar microstructure under a thermal effect, confinement and consequently the strengthening effect no longer holds, which explains the drop of the maximum strength to 40 MPa.

4. Discussion

The high strength and large strain for room temperature deformation combined with high strength at 873 K we report for the Fe–Zr–Cr Laves phase–ferrite composites is remarkable and in full agreement with other recent works (for instance the eutectic Fe–Ti composites [15]). However, in the Fe–Zr–Cr Laves phase–ferrite system, owing to the series of alloys prepared at different cooling rates, we could evidence the key role of the lamellar microstructure scale for both the ambient and high temperature behaviors. The importance of the microstructure scale was already mentioned for several eutectic systems that exhibit high strength–high ductility at room temperature [19, 23]. In the present case, we have noted that the relation between the lamella size and the maximum stress (figure 4(c)) can be consistent with a Hall–Petch-type behavior. Regarding microstructural features, a high density of dislocations is always observed in the ductile phase lamellae after deformation at room temperature. In our previous study [16], for the $\Phi=4$ mm deformed sample, i.e. lamella size $\sim 150\text{--}200$ nm, dislocations were emitted from the Laves phase/ferrite interface and the C14/36 Laves phase lamellae were not sheared. For the $\Phi=2$ mm deformed sample, the lamellae are thinner (~ 100 nm); the dislocation density in these lamellae was too high to allow to observe similar features at the interface only the contrast seems consistent with dislocation nucleation at the interface. However in some areas with smaller lamella size (~ 30 nm), the presence of voids across the lamellae suggests that the C14/36

Laves phase lamellae become shearable below a critical size. This behavior may result from a size effect in the plastic behavior of the C14/36 FeZrCr Laves phases. Indeed, the impact of size reduction on the plastic behavior of some Laves phases has already been evidenced by nanoindentation of micropillars [24]. The main result of the present study is first to reveal the effect of lamella size on the mechanical behavior of the Fe–Zr–Cr Laves phase–ferrite composites. To identify the mechanisms in detail, a dedicated study of the Laves phase/ferrite interface and of the behavior of dislocations as a function of lamella size has to be carried out.

It is worth noting that more information on the deformation mechanism could lead to a better understanding of the high ductility. In composites reinforced by complex metallic phases, it has been reported that strength was increased with a reduction of ductility [18, 25] while other systems exhibit an increase of strength as well as of ductility [26, 27]. The reasons for these different evolutions are not thoroughly identified. The Fe–Zr–Cr composites illustrate rather clearly the possible increase of both ductility and strength due to the reduction of the lamella size. This effect is similar to what was observed in multifilamentary composites [25] and it could be better understood provided more TEM analysis of the interface between the Laves phase and ferrite.

Regarding the high temperature behavior, remarkably the high strength is maintained up to 873 K. In a similar system, Fe-15 wt% Ti alloy with alternate ferrite and Laves phase lamellae [15], a high strength (~ 750 MPa) at 873 K was also reported. In the FeZrCr sample deformed at 873 K, the lamellar microstructure does not show coarsening and the lamella size of the $\Phi=4$ mm sample is still ~ 150 nm. In addition to that our microstructural investigation reveals a high density of dislocations and their propagation in the ferrite lamellae. On the other hand at 1273 K, coarsening has occurred and the microstructure cannot be characterized by a ferrite lamella size anymore. Therefore, it is possible to interpret the high strength at 873 K as a result of the fine lamellar microstructure while the decrease of the strength at higher temperature rather corresponds to the absence of dislocation confinement. At 1273 K, it is not clear whether the Laves phases might also be plastic. High deformability at high temperature for Laves phases and complex metallic phases in general has been frequently reported [1], but there is still no information concerning the Fe–Zr–Cr Laves phases. The TEM study shows that the Laves phase particles in the sample deformed at 1273 K display either a globular or an elongated morphology. However, since coarsening also occurs at 1273 K, it is not possible to conclude from the present observations on a possible deformation of the Laves phases.

In fact for the high temperature behavior, the more noticeable point remains that the microstructure keeps up to 873 K a lamellar microstructure very close to the one at room temperature. Since a high stability under heat treatment is mentioned as a common property of CMA particles like icosahedral phase precipitates [28, 29], it suggests that in CMA phase composites, any strengthening due to the fine scale microstructure existing at ambient temperature could be

somewhat maintained at higher temperature. Indeed, the pronounced softening exhibited by CMA phases [1] can be a drawback for application as a structural material. Therefore, it could be interesting to design composites to avoid a too pronounced softening at high temperature. According to our present work, designing *in situ* composites with a fine scale microstructure can provide interesting solutions to improve both room temperature and high temperature mechanical behavior. In addition to the selection of the CMA phase involved in the composite, the reduction of characteristic scale of the *in situ* composites appears then as a key point to optimize simultaneously several mechanical properties.

5. Conclusion

CMA phases stand as original systems due to their specific atomic decoration and mechanical properties. A way to benefit from their high level of mechanical properties is to develop *in situ* composites of simple alloys and CMA phases. In the present work, we have shown on a very archetypal case (i.e. an *in situ* composites of ferrite and Laves phases) that it was possible to have composites with a very high strength and ductility at ambient temperature and a high strength even at 873 K. In a previous work on similar alloys, microstructural observations had revealed the importance of the Laves phase type (namely C14/36 instead of C15) to improve ductility. Here, the mechanical tests combined with microstructural investigation of deformed samples shows that the increase of strength with reduction of lamella width can be accounted for by the confinement of deformation in ferrite lamellae. Indeed, in the literature, a scale effect was already mentioned for the room temperature mechanical behavior of *in situ* and *ex situ* CMA composites. The present study has made a link between microstructure and mechanical properties which can account for both the room temperature behavior and the possibility of maintaining a high strength at higher temperature. The high strength at 873 K results from the stability of the microstructure or, in other words, on the interface stability specific to *in situ* CMA phase composites.

Acknowledgements

The authors would like to thank B Bartusch, H-J Klauß and H Schulze for technical assistance, and J Das and S Venkataraman for stimulating discussions. This work was supported by the EU within the framework of the European Network of Excellence on Complex Metallic Alloys (NoE CMA).

References

- [1] Dubois J-M, Belin-Ferré E and Feuerbacher M 2010 Introduction to the science of complex metallic alloys *Complex Metallic Alloys: Fundamentals and Applications* ed J-M Dubois and E Belin-Ferré (New York: Wiley-VCH) p 434

- [2] Frank F C and Kasper J S 1958 *Acta Crystallogr.* **11** 184–90
- [3] Sinha A K 1972 *Prog. Mater. Sci.* **15** 81–185
- [4] Steurer W 2007 *Z. Kristallogr.* **222** 259–88
- [5] Weber T, Dshemuchadse J, Kobas M, Conrad M, Harbrecht B and Steurer W 2009 *Acta Crystallogr. B* **65** 308–17
- [6] Pearson P and Cenzual K *Pearson's Crystal Data: Crystal Structure Database for Inorganic Compounds* (Materials Park, Ohio, USA: ASM International)
- [7] Bresson L and Gratias D 1993 *J. Non-Cryst. Solids* **153–154** 468–72
- [8] Machon L and Sauthoff G 1996 *Intermetallics* **4** 469–81
- [9] Bonneville J, Caillard D and Guyot P 2008 Dislocations and plasticity of icosahedral quasicrystals *Dislocations in Solids* vol 14 ed J Hirth (Amsterdam: Elsevier) pp 251–331
- [10] Scudino S, Liu G, Sakaliyska M, Surreddi K B and Eckert J 2009 *Acta Mater.* **57** 4529–38
- [11] Johnson D R, Chen X F, Oliver B F, Noebe R D and Whittenberger J D 1995 *Intermetallics* **3** 141–52
- [12] Zeumer B, Wunnike-Sanders W and Sauthoff G 1995 *Mater. Sci. Eng.: A* **192–193** 817–23
- [13] Palm M, Preuhs J and Sauthoff G 2003 *J. Mater. Process. Technol.* **136** 105–13
- [14] Palm M, Preuhs J and Sauthoff G 2003 *J. Mater. Process. Technol.* **136** 114–9
- [15] Barbier D, Huang M X and Bouaziz O 2013 *Intermetallics* **35** 41–4
- [16] Scudino S, Donnadieu P, Surreddi K B, Nikolowski K, Stoica M and Eckert J 2009 *Intermetallics* **17** 532–9
- [17] Park J M, Sohn S W, Kim T E, Kim D H, Kim K B and Kim W T 2007 *Scr. Mater.* **57** 1153–6
- [18] Park J M, Kim T E, Sohn S W, Kim D H, Kim K B, Kim W T and Eckert J 2008 *Appl. Phys. Lett.* **93** 031913
- [19] Park J M, Kim K B, Kim W T, Lee M H, Eckert J and Kim D H 2008 *Intermetallics* **16** 642–50
- [20] Srivastava R M, Eckert J, Löser W, Dhindaw B K and Schultz L 2002 *Mater. Trans.* **43** 1670–5
- [21] Roisnel T and Rodríguez-Carvajal J 2001 *WinPLOTR Materials Science Forum* **378–381** 118–123
- [22] Stein F, Sauthoff G and Palm M 2002 *J. Phase Equilib.* **23** 480–94
- [23] Das J, Kim K B, Baier F, Löser W and Eckert J 2005 *Appl. Phys. Lett.* **87** 161907
- [24] Korte S and Clegg W J 2012 *Adv. Eng. Mater.* **14** 991–7
- [25] Thilly L, Véron M, Ludwig O and Lecouturier F 2001 *Mater. Sci. Eng.: A* **309–310** 510–3
- [26] Qiao J W, Wang S, Zhang Y, Liaw P K and Chen G L 2009 *Appl. Phys. Lett.* **94** 151905
- [27] Wu F f, Zhang Z f, Peker A, Mao S X, Das J and Eckert J 2006 *J. Mater. Res.* **21** 2331–6
- [28] Nilsson J-O, Stigenberg A H and Liu P 1994 *Metall. Mater. Trans. A* **25** 2225–33
- [29] Liu P, Stigenberg A H and Nilsson J-O 1995 *Acta Metall. Mater.* **43** 2881–90